Chapter 13
Electron Polarimetry

Dave Gaskell

Abstract Electron polarimetry benefits from the ability to use processes with well-known analyzing powers, hence enabling high precision measurements. Several techniques are employed to measure electron beam polarization, including Mott, Møller, and Compton polarimetry. Each technique has particular advantages and disadvantages, depending on the application. This chapter will focus on the techniques used to measure electron beam polarization, with particular emphasis on the challenges and requirements for achieving high precision. The development of a conceptual design of a Compton polarimeter for the future Electron Ion Collider will also be discussed.

13.1 Introduction

Polarized electron beams have been used to great effect in both fixed target accelerators as well as colliders and storage rings. The precision of the electron beam polarization measurement is in general driven by experimental requirements. While measurements providing uncertainties on the order of $dP/P \approx 2-3\%$ are sufficient in many cases, there is an increasing demand for high precision

D. Gaskell (✉)
Experimental Nuclear Physics, Thomas Jefferson National Accelerator Facility, Newport News, VA, USA
e-mail: gaskelld@jlab.org

F. Méot et al. (eds.), *Polarized Beam Dynamics and Instrumentation in Particle Accelerators*, Particle Acceleration and Detection,
https://doi.org/10.1007/978-3-031-16715-7_13

measurements of the polarization, with systematic errors of 1% or better (primarily for experiments employing parity-violating electron scattering such as Q-Weak [1], PREX [2], and the future MOLLER [3] and SoLID [4] experiments). The future Electron Ion Collider (EIC), will require high precision polarimetry (1%) for both electron and hadron beams to fully leverage its expected experimental capabilities.

Typically, three main techniques are used to measure electron beam polarization:

- **Mott Polarimetry** involves the spin-orbit coupling of a (transversely) polarized electron with the Coulomb field of a large Z nucleus. This technique is useful at keV to MeV scale energies—often employed in polarized electron sources or injectors.
- **Møller Polarimetry** makes use of polarized electron-electron scattering. The useful energy range is MeV to 10's of GeV, so can be typically employed at the same beam energy as the experiment. This measurement is usually destructive to the beam due to the ferromagnetic foils used as targets.
- **Compton Polarimetry** employs the scattering of high energy electrons from laser photons. The backscattered photons or scattered electrons (or both) can be used to measure the asymmetry. This technique has the advantage of being non-destructive and can be used for energies larger than $\approx$1 GeV. However, the significant energy dependence of the analyzing power poses certain challenges.

The above techniques are discussed in great detail in Ref. [5], but will be briefly summarized in the sections that follow. It is worth noting that there are additional techniques such as Compton Transmission polarimetry (see for example Refs. [6] and [7]) and so-called "Spin-light" polarimetry [8–10], but these will not be discussed here.

13.2 Mott Polarimetry

Mott polarimetry takes advantage of the asymmetry generated when a transversely polarized electron scatters from an unpolarized large Z nucleus. The asymmetry is generated by the spin-orbit interaction of the electron with the electrostatic field of the nucleus.

The cross section for a polarized electron undergoing Mott scattering at an angle θ is,

$$\sigma(\theta, \phi) = I(\theta)[1 + S(\theta)\overrightarrow{P} \cdot \hat{n}], \tag{13.1}$$

where $I(\theta)$ is the unpolarized cross section, $\overrightarrow{P}$ is the electron polarization, $\hat{n}$ is the unit vector normal to the electron scattering plane, and $S(\theta)$ is the so-called Sherman function, or the Mott scattering analyzing power. The Sherman function is large at

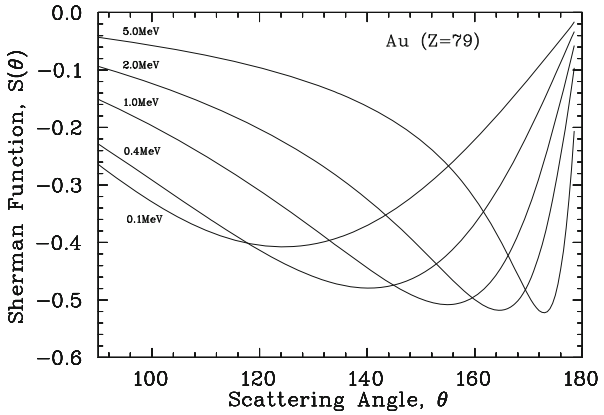

Fig. 13.1 Sherman function for gold vs. Mott scattered electron angle, θ (lab). The Sherman function is larger at backward angles, and at energies of a few MeV approaches its maximum at close to 180 degrees. Figure from Refs. [5, 11]

backward scattering angles, the maximum value occurring at angles approaching 180 degrees at beam energies of a few MeV (see Fig. 13.1).

Some aspects of Mott polarimetry have been described in Sect. 11.8. In general, Mott polarimetry is used in the keV to few MeV range so is typically employed in conjunction with polarized sources. One key advantage of Mott polarimetry is the fact that a polarized target is not required, simplifying experimental aspects of the measurement. On the other hand, the measurement is complicated by the fact that the effective Sherman function for scattering from targets of finite thickness is not the same as the single-atom Sherman function. In the past, this has resulted in systematic uncertainties due to knowledge of the Sherman function estimated to be on the order of 1%. However, recent theoretical and Monte Carlo studies have reduced this uncertainty to $\approx$0.5% resulting in an overall uncertainty of 0.61% [12].

Mott polarimeters are in regular use at CEBAF at Jefferson Lab [12] and at Mainz [13]. While regularly used for checking the performance of the polarized sources, the precision of these polarimeters is such that they are increasingly incorporated in final experimental results.

13.3 Møller Polarimetry

Møller polarimetry measures electron beam polarization using the scattering of polarized electrons from (polarized) atomic electrons in a nucleus. In general, the polarized electrons are generated by applying a magnetic field to a ferromagnetic foil.

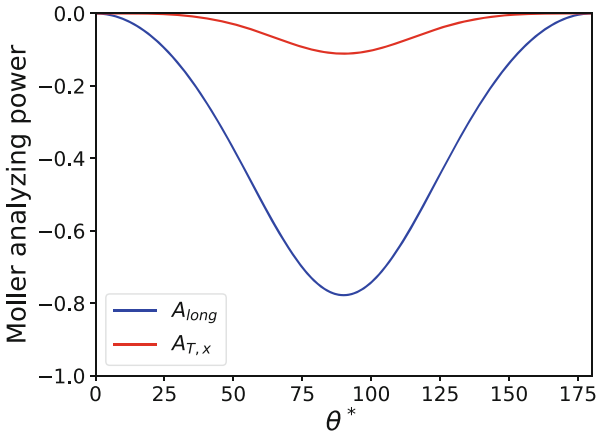

Fig. 13.2 Longitudinal and transverse analyzing powers for Møller scattering vs. center-of-mass scattering angle, θ^*. The analyzing power is maximized at 90 degrees and is $-7/9$ for the longitudinal case, and $-1/9$ for transverse

At energies above 100 MeV, the longitudinal and transverse analyzing powers for polarized Møller scattering are essentially independent of beam energy and are given by,

$$A_{\text{long}} = -\frac{\sin^2\theta^*(7+\cos^2\theta^*)}{(3+\cos^2\theta^*)^2}, \tag{13.2}$$

$$A_{\text{T,x}} = -\frac{\sin^4\theta^*}{(3+\cos^2\theta^*)^2}, \tag{13.3}$$

where A_{long} is the analyzing power for longitudinally polarized beam and target electrons, $A_{\text{T,x}}$ for horizontally polarized beam and target electrons, and θ^* is the center-of-mass scattering angle. Note that the analyzing power is maximized for $\theta^* = 90$ degrees. The longitudinal and transverse Møller analyzing powers are shown in Fig. 13.2.

Møller polarimetry has the advantage of providing rapid and precise beam polarization measurements, but with the caveat that the measurement is generally destructive to the electron beam due to the need to use ferromagnetic foil targets. In addition, Møller measurements are generally limited to rather low beam intensities (a few μA) since beam heating of the target foils leads to target depolarization. Before the late 1990s, most Møller polarimeters used targets slightly tilted with respect to the beam direction with a small applied magnetic field to polarize the electrons in the plane of the foil. This had the disadvantage that the foils were not fully magnetically saturated and the electron polarization had to be inferred from in-situ measurements of the foil magnetization. The group from the University of Basel had the insight that by driving a pure iron foil into magnetic saturation using a 3–4 T applied field, out of plane and parallel to the beam direction, the uncertainties associated with the target polarization (typically at least 2%) could be greatly reduced. A polarimeter using such a target system was built in experimental Hall C at Jefferson Lab with the resulting systematic uncertainty due to target polarization

estimated to be 0.25% [14]. This development opened the door to precision Møller polarimetry, resulting in measurements with systematic uncertainties better than 1%.

Other considerations in the implementation of Møller polarimetry include:

- **Backgrounds:** The primary background in Møller scattering is electron scattering from the atomic nucleus (Mott scattering). This process is easily suppressed by requiring detection of the scattered and recoiling electrons in coincidence.
- **Spectrometer:** A Møller polarimeter requires some sort of magneto-optical system to steer the scattered electrons (which are generally at very small angles in the lab) to the detector system. The spectrometer optics should be designed such that acceptance defining apertures are present only in well-defined, easily understood locations, and ideally, provide the same "tune" or distribution of events at the detectors for a range of beam energies.
- **Acceptance and the Levchuk effect:** It was shown that the distribution of events for more deeply bound (unpolarized) electrons in the atom is different from the outer shell electrons, which carry the majority of the effective target polarization [15]. The Møller polarimeter should have large enough acceptance such that outer and inner shell electrons are detected with nearly the same probability in order to minimize sensitivity to knowledge of the momentum distributions of these electrons.

Recent applications of Møller polarimetry have made an effort to address the above issues, and using a saturated iron foil target have reported results with precision better than 1% [2, 16].

Møller polarimetry is used almost exclusively at fixed-target facilities such as SLAC, MAMI, and Jefferson Lab. Application in a storage ring would require the development of a non-destructive target. A target based on atomic hydrogen stored in a cold magnetic trap is being pursued at Mainz for the P2 experiment. There is some question as to whether such a target would remain polarized at the high beam intensities generally used in a storage ring. A jet target would be another potential alternative, and some initial tests of Møller polarimetry using such a target were performed at VEPP3 [17], although further work would be required to determine the ultimate precision that could be achieved.

13.4 Compton Polarimetry

A Compton polarimeter measures electron beam polarization via the collision of circularly polarized laser light of energy ∼few eV with high energy electrons. The backscattered photon energy (E_γ) is significantly larger than the laser photon energy (E_{laser}), and is proportional to the relativistic gamma factor (squared) of the incoming electron:

$$E_\gamma = E_{laser} \frac{4a\gamma^2}{1 + a\theta_\gamma^2 \gamma^2}, \tag{13.4}$$

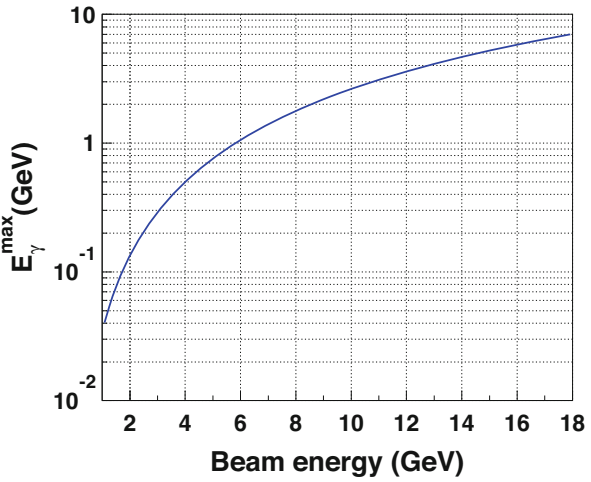

Fig. 13.3 Maximum Compton backscattered photon energy vs. initial electron beam energy for a 532 nm (green) laser

where $\gamma = E_e/m_e$ (with E_e and m_e the electron energy and mass) and $a = (1 + 4\gamma E_{laser}/m_e)^{-1}$. The backscattered photon energy as a function of electron beam energy at the kinematic endpoint (180-degree scattering) for a green, 532 nm laser is shown in Fig. 13.3.

The Compton analyzing power for longitudinally polarized electrons depends only on the backscattered photon energy and is given by,

$$A_{\text{long}} = \frac{2\pi r_o^2 a}{(d\sigma/d\rho)}(1 - \rho(1 + a))\left[1 - \frac{1}{(1 - \rho(1 - a))^2}\right], \tag{13.5}$$

where r_o is the classical electron radius, ρ is the backscattered photon energy divided by its kinematic maximum, E_γ/E_γ^{max}, and $d\sigma/d\rho$ is the unpolarized Compton cross section. The transverse analyzing power depends both on the backscattered photon energy and the azimuthal angle (ϕ) between the electron polarization direction and the backscattered photon,

$$A_{\text{T}} = \frac{2\pi r_o^2 a}{(d\sigma/d\rho)} \cos\phi \left[\rho(1 - a)\frac{\sqrt{4a\rho(1 - \rho)}}{(1 - \rho(1 - a))}\right]. \tag{13.6}$$

This dependence on the azimuthal angle results in an asymmetry that depends on the location of the backscattered photon. For example, a vertically polarized electron beam would result in an "up-down" asymmetry. The longitudinal and transverse analyzing powers are shown in Fig. 13.4.

A basic Compton polarimeter requires a laser system, a dipole to deflect the electron beam away from the path of the backscattered photons, and a detector system for those photons. The scattered electrons are momentum-analyzed in the same dipole and those electrons are then separated from the beam, which allows the use of a position sensitive electron detector.

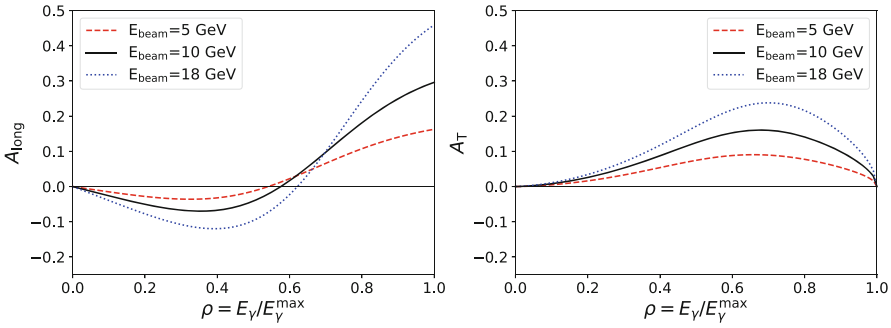

Fig. 13.4 Compton longitudinal (left) and transverse (right) analyzing power as a function of relative backscattered photon energy, ρ. The analyzing power is shown for 5,10, and 18 GeV electrons assuming a 532 nm (green) laser. The transverse asymmetry is evaluated at $\phi = 0$

Some considerations for the application of Compton polarimetry include:

- The beam intensity and duty cycle of the electron beam will impact the choice of laser system. For example, the relatively low intensity of the beam at Jefferson lab requires a laser with a resonating Fabry-Perot cavity. The intensity and duty cycle will also determine the measurement technique. A low duty-cycle beam may require measurements in so-called multi-photon mode, in which several backscattered photons (or scattered electrons) are generated from the laser collision with each beam bunch.
- The beam energy will impact the choice of laser wavelength - a shorter wavelength is desirable at lower energies, where the analyzing power is smaller.
- The beam polarization direction (longitudinal or transverse) will dictate the type of detector required. For example, for measurements of the longitudinal polarization, the photon detector need only measure the total energy of the backscattered photon, but for the transverse case, one must measure the position as well.

Most Compton polarimeters constructed in recent years have been used to measure the longitudinal beam polarization. The highest precision device was used in the SLD experiment at SLAC and quoted a systematic uncertainty of dP/P=0.52% at 45.6 GeV [18]. The SLD Compton measured the scattered electrons in multi-event (integrating) mode using a segmented gas Cherenkov detector. Jefferson Lab has Compton polarimeters in experimental Halls A and C, achieving systematic errors of 0.59% in Hall C [19] (using a diamond strip electron detector) and 1% in Hall A [20, 21] (using a silicon strip electron detector operated in single-event mode and a photon calorimeter operated in integrating mode). Longitudinal Compton polarimeters have also been implemented at MIT-Bates, NIKHEF, and HERA. In addition to the longitudinal polarimeter, HERA also deployed a transverse Compton, one of the few transverse Compton polarimeters intended to provide relatively precise absolute measurements of the beam polarization. In the end, the final

systematic uncertainty for this device was 2.9% [22]. It is worth noting that the EIC will require measurement of the degree of transverse as well as longitudinal electron polarization and as one of the few examples of transverse Compton polarimetry, the HERA TPOL provides useful lessons for implementation at EIC.

13.5 Polarimetry for EIC

The Electron Ion Collider will be the first collider with both polarized hadrons and electrons, and the high luminosity will allow extremely high statistical precision for a range of processes (DIS, SIDIS, and exclusive reactions) over a large kinematic range. It is crucial that the experimental systematic uncertainties are also under control to fully leverage the capabilities of the EIC. Specifically, the systematic uncertainty goal for polarimetry (for both electrons and hadrons) is dP/P=1%.

The EIC layout is shown in Fig. 13.5. The electrons are generated with full polarization at the electron source, accelerated to 400 MeV in the Injector Linac, and then enter the Rapid Cycling Synchrotron (RCS) where they are accelerated to the full beam energy (5 to 18 GeV). From the RCS, electron bunches enter the Electron Storage Ring (ESR) where they interact with the hadron bunches at the experimental area at IR6. Mott polarimetry will be used at the polarized source, measurements of the polarization are planned just after the RCS (Møller and Compton polarimetry are both being studied), and a Compton polarimeter will be used in the Electron Storage Ring. The discussion here will focus on the conceptual design of the ESR Compton polarimeter. Note that since the design of the EIC is still ongoing, the final configuration of the EIC Compton polarimeter may differ from what is presented here.

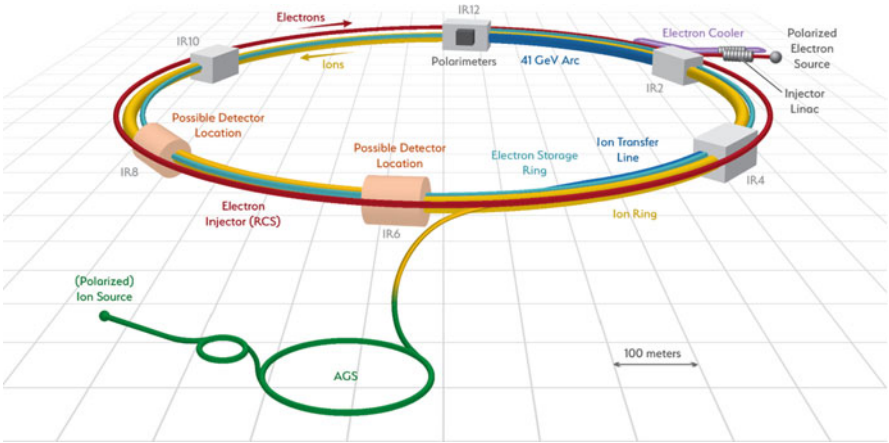

Fig. 13.5 Layout of the Electron Ion Collider. Electrons start at the polarized source (3 o'clock), are accelerated to full energy in the RCS (red ring) and then injected into the ESR

Table 13.1 EIC electron beam properties at 5, 10, and 18 GeV

Beam property	5 GeV	10 GeV	18 GeV
Bunch frequency	99 MHz	99 MHz	24.75 MHz
Pulse width	63.3 ps	63.3 ps	30 ps
Intensity (average)	2.5 A	2.5 A	0.227 A
Bunch lifetime	>30 min.	>30 min.	6 min
P_L at IR6 Compton location	97.6%	90.7%	70.8%
P_T at IR6 Compton location	21.6%	42.2%	70.6%

The design of the ESR Compton polarimeter depends on the electron beam properties as well as the polarimeter requirements. The main requirements of the EIC Compton in the ESR are:

- Measurement of the electron polarization bunch-by-bunch
- Compton rates sufficient to make a 1% (statistical) measurement in a time shorter than the bunch lifetime
- The ability to measure all components (longitudinal and transverse) of the electron beam polarization
- Systematic errors of 1% or better

The EIC electron beam properties are summarized in Table 13.1. The high bunch frequency (24.75–99 MHz) and the requirement to measure the electron beam polarization for each bunch pose the first significant challenge. The small time between bunches (about 10 ns at 5 and 10 GeV) means that the Compton detectors and laser system must have very fast time response. While the high average intensity of the beam has benefits for making rapid measurements, it also implies larger than average backgrounds, especially synchrotron radiation. In addition, due to lack of space, the polarimeter cannot be placed at the experiment at IR6, so there will be some spin precession between the Compton location and the experiment. This means that in order to extract the absolute polarization with high precision, the polarimeter must be designed to have small systematic errors for both longitudinal and transverse polarization measurements simultaneously.

The layout of the Compton polarimeter at its proposed location upstream of IR6 is shown in Fig. 13.6. As seen in the figure, the laser enters the beamline vacuum downstream of the 3rd dipole in the section shown, and interacts with the electron beam at the location of the quadrupole between the 2nd and 3rd dipoles. The backscattered photon detector will be about 20–30 meters downstream of the Compton interaction point while the electron detector will be closer since the large dispersion introduced by the dipole results in sufficient spatial separation of the scattered electrons without as much drift.

The main elements of the ESR Compton polarimeter are described in more detail in the EIC Yellow Report [23], but are summarized briefly here.

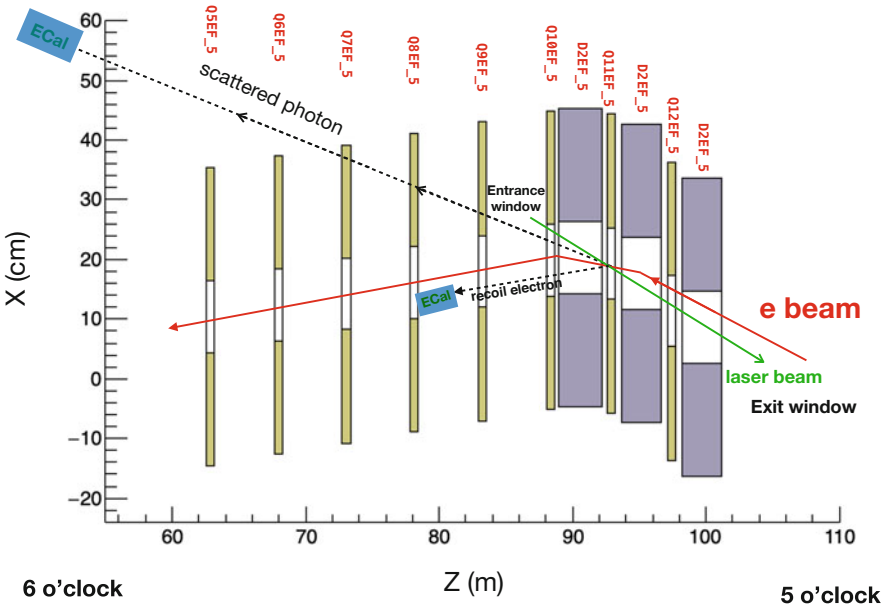

Fig. 13.6 Layout of the ESR Compton polarimeter, upstream of IR6. The elements labeled D2EF_5 denote dipoles, while the elements labeled QxEF_5 (where x=5-12) are quadrupoles

Laser System

The ideal laser system for the Compton polarimeter would be a pulsed laser with the same repetition rate and similar pulse width as the electron bunches. While pulsed lasers at 100 MHz are readily available using commercial mode-locked systems, these lasers lack flexibility and multiple systems would be required for operation at 99 and 24.75 MHz. Instead, the planned system for the EIC Compton makes use of a gain-switched diode laser, operated at a frequency determined by an RF source. Such diode lasers are readily commercially available and are relatively inexpensive. The gain-switched diode (providing light at 1064 nm) is then amplified using fiber amplifiers and subsequently frequency doubled to 532 nm.

Luminosity calculations indicate that an average power of 5–10 W is sufficient to generate one backscattered photon per laser-electron bunch crossing. Since the polarimeter will operate in single event counting mode, higher luminosity is not required.

This system is similar to laser systems that have been used at Jefferson Lab in the injectors for the CEBAF accelerator and Low Energy Recirculator Facility (LERF) with much success and have demonstrated great reliability. The fact that the system is modular (seed laser, fiber amplifier, doubling system) is also a benefit in that it facilitates easier repair.

Position Sensitive Detectors

Position sensitive detectors are required for both the scattered electrons and the backscattered photons. As noted earlier, the scattered electrons are momentum-analyzed in the 3rd dipole such that electrons of different energy are spread out in the horizontal direction. A horizontally segmented detector allows the determination of the electron energy, and the asymmetry vs. energy can be extracted for determination of the longitudinal polarization. Studies have shown that reliable determination of the polarization requires at least 30 bins in energy between the asymmetry zero-crossing and the kinematic endpoint. For the configuration at EIC, this implies a required segmentation of about 400 μm. Note that the electron detector will not be sensitive to the degree of transverse polarization since the transverse electron spin direction will also be in the horizontal plane, resulting in a left-right asymmetry. This left-right asymmetry cannot be extracted due to energy dispersion of the 3rd dipole.

The photon detector, on the other hand, has no such issue and will be used to measure the degree of transverse electron polarization via the left-right asymmetry. In principle, one must know the horizontal position of the photon detector relative to the beam-laser collision point to accurately fit the left-right asymmetry. However, with sufficient detector position resolution, one can allow the asymmetry zero-crossing position to float in the fit, making extraction of the polarization insensitive to the detector position. Studies indicate that a segmentation of about 100 μm is sufficient for a detector placed 20 m from the Compton-electron IP (see Fig. 13.7).

Diamond strip detectors are an excellent candidate for both the electron and photon position sensitive detectors. The required segmentation is readily achievable

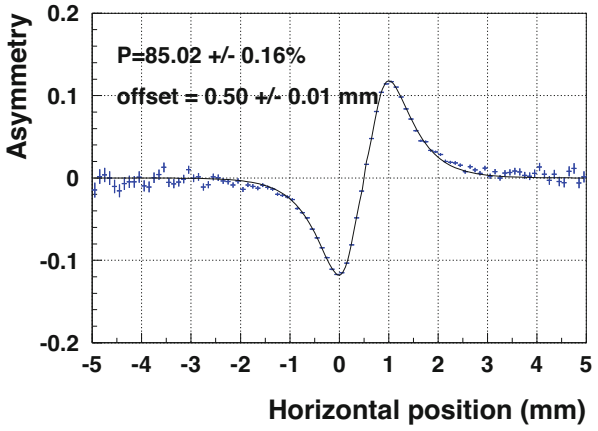

Fig. 13.7 Simulated transverse electron asymmetry at the position of the photon detector (20 m from the Compton-electron IP) vs. horizontal position. In this example, the detector has been deliberately offset by 0.5 mm, but the fit still results in the correct beam polarization (85.0%) when using bin sizes of 100 μm and including the offset as a parameter in the fit

and diamond detectors have the advantage of being very radiation hard. In addition, diamond has been shown to have response times compatible with the 10 ns spacing of the EIC electron bunches, although some development is likely required for the amplification and readout electronics.

Photon Calorimeter
A calorimeter is required to measure the energy of the backscattered photon. Radiation hardness, good energy resolution, and fast time response are desirable. Although lead-tungstate has good energy resolution and is relatively radiation hard, there is a mix of fast and slow time components in the detector response that may make such a detector incompatible with the 10 ns bunch structure. A tungsten-powder calorimeter is also under consideration, but its energy resolution is worse than lead-tungstate which may result in larger systematic uncertainties. Detailed Monte Carlo simulations will be required to determine if the tungsten-powder response is adequate.

13.6 Summary

In contrast to hadron polarimetry, there are several processes available which allow the measurement of the absolute polarization of electrons. Mott, Møller, and Compton polarimetry are the most frequently used techniques and all three have areas in which they are optimal. Precision measurements in the field of parity violating electron scattering have been the primary motivation for recent improvements in electron beam polarimetry. Although not discussed in detail here, direct comparisons of different devices using different techniques have played an important role in demonstrating the reliability of polarization measurements and have helped identify previously unknown systematic uncertainties [24]. Electron beam polarimetry will also be crucial to the success of the EIC program—achieving the needed performance of the Compton polarimeter in the EIC electron storage ring will pose unique challenges that require further developments.

Acknowledgments This material is based upon work supported by the U.S. Department of Energy, Office of Science, Office of Nuclear Physics under contracts DE-AC05-06OR23177.

References

1. D. Androić et al., Nature **557**, 7704, 207–211 (2018). https://doi.org/10.1038/s41586-018-0096-0 [arXiv:1905.08283 [nucl-ex]]
2. D. Adhikari et al., Phys. Rev. Lett. **126**(17), 172502 (2021) https://doi.org/10.1103/PhysRevLett.126.172502 [arXiv:2102.10767 [nucl-ex]]
3. J. Benesch et al., Nucl. Exp. (2014) [arXiv:1411.4088 [nucl-ex]]
4. J.P. Chen et al., Nucl. Exp. (2014) [arXiv:1409.7741 [nucl-ex]]

5. K. Aulenbacher, E. Chudakov, D. Gaskell, J. Grames, K.D. Paschke, Int. J. Mod. Phys. E **27**(07), 1830004 (2018). https://doi.org/10.1142/S0218301318300047
6. C. Weinrich, Eur. Phys. J. A **24S2**, 129–130 (2005) https://doi.org/10.1140/epjad/s2005-04-030-2
7. R. Barday, K. Aulenbacher, P. Bangert, J. Enders, A. Gook, D.H. Jakubassa-Amundsen, F. Nillius, A. Surzhykov, V.A. Yerokhin, J. Phys. Conf. Ser. **298**, 012022 (2011) https://doi.org/10.1088/1742-6596/298/1/012022
8. I.P. Karabekov, R. Rossmanith, *Proceedings of International Conference on Particle Accelerators* https://doi.org/10.2172/10186698
9. I.P. Karabekov, S.I. Karabekian, Conf. Proc. C **960610**, 1743–1745 (1996)
10. P. Mohanmurthy, D. Dutta, PoS **PSTP2013**, 038 (2013). https://doi.org/10.22323/1.182.0038 [arXiv:1401.6744 [physics.acc-ph]]
11. Under a Creative Commons license. https://creativecommons.org/licenses/by/4.0/
12. J.M. Grames, C.K. Sinclair, M. Poelker, X. Roca-Maza, M.L. Stutzman, R. Suleiman, M.A. Mamun, M. McHugh, D. Moser, J. Hansknecht, et al., Phys. Rev. C **102**(1), 015501 (2020). https://doi.org/10.1103/PhysRevC.102.015501
13. V. Tioukine, K. Aulenbacher, E. Riehn, Rev. Sci. Instrum. **82**(3), 033303 (2011). https://doi.org/10.1063/1.3556593
14. M. Hauger, A. Honegger, J. Jourdan, G. Kubon, T. Petitjean, D. Rohe, I. Sick, G. Warren, H. Wohrle, J. Zhao, et al., Nucl. Instrum. Meth. A **462**, 382–392 (2001). https://doi.org/10.1016/S0168-9002(01)00197-8 [arXiv:nucl-ex/9910013 [nucl-ex]]
15. L.G. Levchuk, Nucl. Instrum. Meth. A **345**, 496–499 (1994). https://doi.org/10.1016/0168-9002(94)90505-3
16. J.A. Magee, A. Narayan, D. Jones, R. Beminiwattha, J.C. Cornejo, M.M. Dalton, W. Deconinck, D. Dutta, D. Gaskell, J.W. Martin, et al., Phys. Lett. B **766**, 339–344 (2017) https://doi.org/10.1016/j.physletb.2017.01.026 [arXiv:1610.06083 [physics.ins-det]]
17. A.V. Grigoriev, V. Kiselev, E.V. Kremyanskaya, E. Levichev, S.I. Mishnev, S.A. Nikitin, D.M. Nikolenko, I.A. Rachek, Y.V. Shestakov, D.K. Toporkov, et al., *Proceedings of EPAC 2004*. EPAC-2004-THPLT106
18. M. Woods, High Energy Phys. - Exp. [arXiv:hep-ex/9611005 [hep-ex]]
19. A. Narayan, D. Jones, J.C. Cornejo, M.M. Dalton, W. Deconinck, D. Dutta, D. Gaskell, J.W. Martin, K.D. Paschke, V. Tvaskis, et al., Phys. Rev. X **6**(1), 011013 (2016). https://doi.org/10.1103/PhysRevX.6.011013 [arXiv:1509.06642 [nucl-ex]]
20. A. Acha et al., Phys. Rev. Lett. **98**, 032301 (2007). https://doi.org/10.1103/PhysRevLett.98.032301 [arXiv:nucl-ex/0609002 [nucl-ex]]
21. M. Friend, D. Parno, F. Benmokhtar, A. Camsonne, M. Dalton, G.B. Franklin, V. Mamyan, R. Michaels, S. Nanda, V. Nelyubin, et al., Nucl. Instrum. Meth. A **676**, 96–105 (2012) https://doi.org/10.1016/j.nima.2012.02.041 [arXiv:1108.3116 [physics.ins-det]]
22. B. Sobloher, Phys.: Instrum. Detect. [arXiv:1201.3836 [physics.ins-det]]
23. R. Abdul Khalek, A. Accardi, J. Adam, D. Adamiak, W. Akers, M. Albaladejo, A. Al-bataineh, M.G. Alexeev, F. Ameli, P. Antonioli, et al., Phys.: Instrum. Detect. [arXiv:2103.05419 [physics.ins-det]]
24. J.M. Grames, C.K. Sinclair, J. Mitchell, E. Chudakov, H.C. Fenker, A. Freyberger, D.W. Higinbotham, M. Poelker, M. Steigerwald, M. Tiefenback, et al., Phys. Rev. ST Accel. Beams **7**, 042802 (2004) [erratum: Phys. Rev. ST Accel. Beams **13**, 069901 (2010)] https://doi.org/10.1103/PhysRevSTAB.7.042802